



## ADSORPTION STUDY OF METHYL ORANGE DYE USING Co/Fe-CO<sub>3</sub> HYDROTALCITE

Dian Windy Dwiasi<sup>1</sup>, Alya Destia Ramadhani<sup>1\*</sup>, Ely Setiawan<sup>1</sup>

<sup>1</sup> Department of Chemistry, Jenderal Soedirman University,  
Purwokerto, Central Java, Indonesia, 53123

Email : alyades2012@gmail.com

**Abstract.** Methyl orange is a hazardous anionic dye for the environment; hence, it is necessary to carry out processing before disposal. One of the methods for its treatment is adsorption. Hydrotalcite is used as an adsorbent due to its significant adsorption capacity. This research aims to study the adsorption of methyl orange using Co/Fe-CO<sub>3</sub> hydrotalcite, with test parameters including pH, contact time, adsorbent mass, methyl orange concentration, and to determine the kinetic and isotherm adsorption models. The synthesis of Co/Fe-CO<sub>3</sub> hydrotalcite is conducted through coprecipitation with a 4:1 mole ratio of Co<sup>2+</sup> ions to Fe<sup>3+</sup> ions, followed by hydrothermal treatment at 65°C for 24 hours. Hydrotalcite was characterized using FTIR and XRD. The optimum conditions for methyl orange adsorption by Co/Fe-CO<sub>3</sub> hydrotalcite are obtained at pH 6, a contact time of 60 minutes, an adsorbent mass of 50 mg, and a methyl orange concentration of 80 mg/L. The adsorption kinetics followed pseudo-second-order dynamics with an R<sup>2</sup> value of 0.9998; the adsorption rate constant is 0.025 g/mg.minute, and the q<sub>e</sub> value is 13.793 mg/g. The adsorption isotherm model followed the Freundlich isotherm model, with R<sup>2</sup>, n, KF, and E values of 0.9969, 3.073 mg/g, and -2.781 kJ/mol, respectively.

**Keywords:** B. gymnorhiza, carboxymethyl chitosan, nanoparticles, ionic gelation

### 1. Introduction

The textile industry is one of the contributors of liquid waste generated from the dyeing process. One of the dyes widely used in the textile industry is methyl orange. This dye consists of azo groups and its derivatives, particularly benzene groups, which are known to be highly resistant to degradation. Therefore, a treatment is required to reduce the concentration of methyl orange in wastewater to make it environmentally safe.

Adsorption is widely recognized as an effective method for dye removal from water, primarily due to its cost-effectiveness, operational simplicity, and scalability. Activated carbon is a renowned adsorbent in wastewater treatment, exhibiting exceptional adsorption capabilities for color, odor, oil, and toxic organic pollutants [1]. Nonetheless, the operational cost of activated carbon adsorption is high, and its regeneration process is challenging. Therefore, it is imperative to explore alternative materials with potential adsorption properties, such as hydrotalcite.

Hydrotalcite, an anionic clay with stacked positive layers and interlayer anions, offers several advantages, including a substantial surface area, anion exchange capabilities, and ease of synthesis [2]. Synthesis of Ni/Fe-NO<sub>3</sub> hydrotalcite for the adsorption of the dye methyl orange (MO) and the metal Cr(VI), demonstrating significant adsorption capacities of 205.76 mg/g for MO and 26.78 mg/g for Cr(VI) [3]. Another research is synthesized Co/Fe-CO<sub>3</sub> hydrotalcite for the adsorption of wastewater containing complex chromium [4].

Based on the aforementioned studies, hydrotalcite shows great potential as an effective adsorbent due to its high adsorption capacity. Therefore, this research focuses on the adsorption study of Co/Fe-CO<sub>3</sub> hydrotalcite for the removal of methyl orange dye. Hydrotalcite with carbonate ions as interlayer anions is known to be challenging to exchange due to its strong affinity [5]. The adsorption study includes parameters such as pH, contact time, adsorbent dosage, and the maximum dye concentration to determine the kinetics and adsorption isotherms. This will provide insights into the adsorption capability of Co/Fe-CO<sub>3</sub> hydrotalcite as a methyl orange dye adsorbent.

## 2. Methods

### 2.1. Tools and Materials

The tools used in this study were an analytical balance, magnetic stirrer, oven, Whatman No. 42 filter paper with a diameter of 90 mm, pH meter, glassware, volumetric flask, Eppendorf tubes, watch glasses, dropper pipettes, volumetric pipettes, filler, centrifuge, and shaker. In addition, the instruments used are a UV-Vis spectrophotometer, X-ray Diffractometer (with CuK $\alpha$  radiation source,  $\lambda = 0.15406$  nm, operating conditions at 40 kV and 30 mA,  $2\theta = 2^\circ - 60^\circ$  at room temperature), and Infrared Spectrophotometer. Whereas, the materials used in this study were methyl orange p.a, cobalt nitrate (Co(NO<sub>3</sub>)<sub>2</sub>·6H<sub>2</sub>O) p.a, iron(III) nitrate (Fe(NO<sub>3</sub>)<sub>3</sub>·9H<sub>2</sub>O) p.a, sodium hydroxide (NaOH) p.a, sodium carbonate (Na<sub>2</sub>CO<sub>3</sub>) p.a, nitric acid (HNO<sub>3</sub>) p.a, pH paper, nitrogen gas, distilled water, and deionized water.

### 2.2. Synthesis and characterization of Co/Fe-CO<sub>3</sub> hydrotalcite

A cobalt/iron carbonate layered double hydroxide with a cobalt–iron ratio of 4:1 was used in this study. The Co/Fe-CO<sub>3</sub> hydrotalcite was synthesised using the co-precipitation method. A total of 11.64 grams of Co(NO<sub>3</sub>)<sub>2</sub>·6H<sub>2</sub>O and 4.04 grams of Fe(NO<sub>3</sub>)<sub>3</sub>·9H<sub>2</sub>O were separately dissolved in 100 mL of deionized water each. The solutions were mixed while continuously purged with nitrogen gas and stirred using a magnetic stirrer for 30 minutes. Solution B was prepared by mixing 0.4M Na<sub>2</sub>CO<sub>3</sub> and 0.96M NaOH, each in 50 mL of deionized water. Solution A was then slowly added drop by drop into Solution B under magnetic stirring. During the reaction, the pH of the reaction system was carefully maintained at approximately 10.0. Subsequently, following the reaction, the mixture was aged at 65°C for 24 hours. Afterward, the sediment was subjected to multiple washes until the supernatant reached a neutral pH. The washed sediment was then dried at 65°C for 18 hours and subsequently ground into a fine powder. The resulting powder was identified as Co/Fe-CO<sub>3</sub>, and then this powder was characterized using FTIR and XRD to determine its characteristics.

### 2.3. Adsorption Experiments

#### 2.3.1 Preparation of Methyl Orange Stock Solution

A total of 0.1 grams of methyl orange was dissolved in a 100 mL volumetric flask and then topped up with distilled water to the mark. This solution had a concentration of 1000 ppm. The stock solution was used to prepare standard solutions through a series of dilutions.

#### 2.3.2 Preparation of Methyl Orange Calibration Curve

The calibration curve was constructed by plotting the relationship between concentration (x) and absorbance (y) to obtain the linear regression equation  $y = bx + a$ . This

regression equation was used to determine the concentration of adsorbed methyl orange in the samples. A 100 ppm methyl orange stock solution was prepared, and various concentrations of 2, 4, 6, 8, 10, and 12 ppm were derived from it. The absorbance of each solution was measured using a UV-Vis spectrophotometer at the maximum wavelength.

### 2.3.3 Effect of pH

The adsorption experiments were carried out by a batch method in an open medium and at room temperature. A total of 16 mL of 10 ppm methyl orange solution was prepared at varying pH levels from 4 to 12 using NaOH and HNO<sub>3</sub> solutions. Then, 0.01 grams of the adsorbent were added to each solution. The mixtures were homogenized using a shaker for 1 hour. The solution was separated from the adsorbent by centrifugation at a speed of 2500 rpm, and the filtrate was analyzed using a UV-Vis spectrophotometer to determine the concentration of methyl orange.

### 2.3.4 Effect of contact time

A total of 16 mL of 10 ppm methyl orange solution was adjusted to the optimum pH. Then, 0.01 grams of the adsorbent were added to the solution, and it was homogenized using a shaker for various time intervals, namely, 5, 10, 15, 30, 40, 50, 60, 70, 80, 90, 120, 150, and 180 minutes. The solution was separated from the adsorbent by centrifugation at a speed of 2500 rpm, and the filtrate was analyzed using a UV-Vis spectrophotometer to determine the concentration of methyl orange.

### 2.3.5 Effect of LDH amount

A total of 16 mL of 10 ppm methyl orange solution was added with hydrotalcite with weight variation of 0.01 grams to 0.09 grams at the optimum pH. The mixture was then homogenized for the optimal contact time. The solution was separated from the adsorbent by centrifugation at a speed of 2500 rpm, and the filtrate was analyzed using a UV-Vis spectrophotometer to determine the concentration of methyl orange.

### 2.3.6 Effect of methyl orange concentration

A total of 16 mL of methyl orange solution was made with varying concentrations of 10 - 100 ppm at optimum pH, adding hydrotalcite with optimum weight. The mixture was homogenized using a shaker at the optimum contact time. The solution was separated from the adsorbent by centrifugation at a speed of 2500 rpm, then the filtrate was analyzed using a UV-Vis spectrophotometer so that the methyl orange content could be determined.

### 2.3.7 Adsorption kinetic

The data obtained from the adsorption process in determining the optimum contact time were utilized to determine the adsorption reaction kinetics using first-order (1), second-order (2), pseudo-first-order (3), and pseudo-second-order (4) equations

$$\ln C_t = -k_1 \cdot t + \ln C_0 \quad (1)$$

$$\frac{1}{C_t} = k_2 \cdot t + \frac{1}{C_0} \quad (2)$$

$$\log(q_e - q_t) = \log q_e - \frac{k_1 t}{2.303} \quad (3)$$

$$\frac{t}{q_t} = \frac{1}{k_2 q_e^2} + \frac{1}{q_e} \quad (4)$$

### 2.3.8 Adsorption isotherm

The adsorption data obtained in the determination of the optimum concentration are used to determine the type of adsorption isotherm. The determination of the Langmuir adsorption isotherm is based on Equation (5).

$$\frac{C_e}{q_e} = \frac{1}{q_{maks}} C_e + \frac{1}{K_L \cdot q_{maks}} \quad (5)$$

Meanwhile, the determination of the Freundlich adsorption isotherm type is based on Equation (6).

$$\ln q_e = \frac{1}{n} \ln C_e + \ln K_F \quad (6)$$

### 3. Results And Discussion

#### 3.1. Co/Fe-CO<sub>3</sub> hydrotalcite

Hydrotalcite Co/Fe-CO<sub>3</sub> with a Co/Fe molar ratio of 4:1 was synthesized using the coprecipitation method. This molar ratio was chosen based on the research [6], which showed increased crystallinity in Co/Fe hydrotalcite with a higher Co<sup>2+</sup> content. This indicates that an increased cation ratio results in materials with high crystallinity and a large surface area.

The preparation of Co/Fe-CO<sub>3</sub> hydrotalcite started with the preparation of solution A and solution B containing interlayer anions. Solution A was prepared by mixing solutions of Co(NO<sub>3</sub>)<sub>2</sub>·6H<sub>2</sub>O and Fe(NO<sub>3</sub>)<sub>2</sub>·9H<sub>2</sub>O, resulting in a red-colored solution, while solution B was prepared by mixing solutions of NaOH and Na<sub>2</sub>CO<sub>3</sub>, resulting in a clear solution. Solution A was added to solution B under rapid and constant stirring for 2 hours. During the reaction, the pH of the system was maintained at pH 10 using NaOH.

After mixing, a brown slurry was formed. The slurry was then placed in a Teflon container and subjected to hydrothermal treatment at 65°C for 24 hours. The time and temperature in this process produced Co/Fe-CO<sub>3</sub> hydrotalcite sheets with a large surface area [7]. After hydrothermal treatment for 24 hours, the slurry was filtered and washed with deionized water until reaching pH 7. The obtained precipitate was then dried at 65°C for 18 hours to remove residual water in the hydrotalcite. Drying conditions [8] showed that using low temperature and longer drying time results in crystals with a large surface area. The resulting Co/Fe-CO<sub>3</sub> hydrotalcite adsorbent is in the form of brown solid particles.

#### 3.2. Characterization of materials

##### 3.2.1 XRD analysis

Hydrotalcite synthesized products were characterized using X-ray diffractometer to identify that the main compound of the synthesis product is Co/Fe-CO<sub>3</sub> hydrotalcite. Figure 4.1 displays the characteristic diffraction peaks of the synthesized Co/Fe-CO<sub>3</sub> hydrotalcite located at 2θ values of 11.454°, 23.184°, 33.919°, 38.558°, and 59.069°. These diffraction peaks closely resemble those of the standard Co/Fe hydrotalcite structure (JCPDS No. 50-0235).

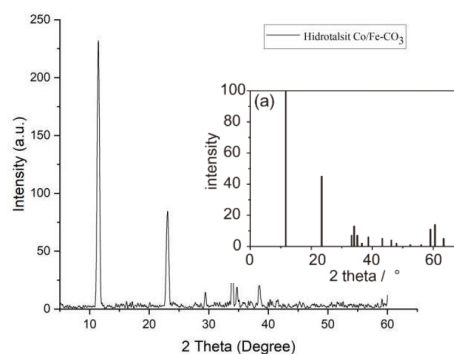


**Figure 1.** XRD patterns of Co/Fe-CO<sub>3</sub> hydrotalcite

The characteristic peak at  $2\theta = 11.454^\circ$  indicates the presence of carbonate anions in the interlayer of the synthesized hydrotalcite with a basal spacing of 7.72 Å. This finding is in line with the research [9], which reported carbonate anion reflections on the (003) plane at 7.57 Å and 7.67 Å. The sharp and symmetric diffraction peaks at low  $2\theta$  values suggest that the hydrotalcite phase has crystallized well. Increased cobalt content in the hydrotalcite structure leads to greater stability and an increase in interlayer spacing. Conversely, higher iron content can disrupt the layer structure of hydrotalcite and reduce its crystallinity [10].

### 3.2.2 FTIR

The hydrotalcite material was characterized using a FTIR (Fourier-Transform Infrared) spectrophotometer to complement the synthesis data by identifying the functional groups present in the hydrotalcite compound. The FTIR spectrum of the hydrotalcite obtained in this study is shown in Figure 2.

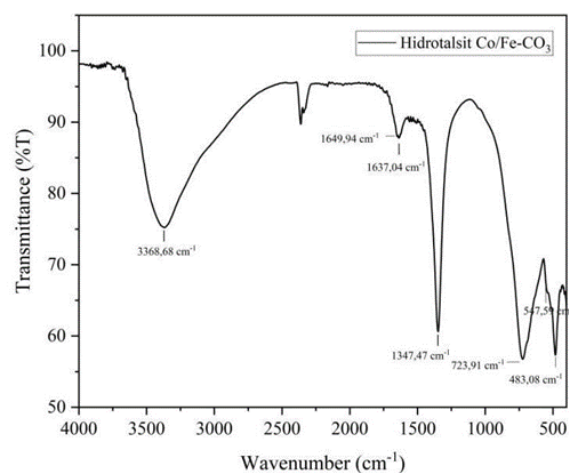


**Figure 2.** FTIR spectrum of Co/Fe-CO<sub>3</sub> hydrotalcite

The FTIR analysis was conducted in the wavenumber range of 4000-400 cm<sup>-1</sup>. Based on Figure 2, the Co/Fe-CO<sub>3</sub> hydrotalcite exhibits broad absorptions at wavenumbers of 3368.68 cm<sup>-1</sup>, which correspond to the stretching vibration of O-H groups from water molecules in the interlayer of the hydrotalcite. Furthermore, the absorption at 1637.04 cm<sup>-1</sup> arises from the bending vibration of O-H groups within water molecules in the interlayer region. Additional absorptions are observed at wavenumbers 1347.47 cm<sup>-1</sup> and 1649.49 cm<sup>-1</sup>, indicating the stretching vibration of C-O and the vibration of C=O groups from CO<sub>3</sub><sup>2-</sup> anions. Absorptions around 547.59 cm<sup>-1</sup> and 483.08 cm<sup>-1</sup> in the low wavenumber region are associated with the brucite-like structure, believed to originate from the M-O and M-O-M (M = Co, Fe) vibrations within the layered metal hydroxide sheets.

### 3.3. Adsorption study

#### 3.3.1 Calibration curve

The calibration curve is a line that represents the relationship between concentration and absorbance values. The calibration curve generated can be used to demonstrate the linear relationship between the actual substance concentration and the instrument's response. Linearity between concentration and absorbance is expressed in the correlation coefficient (R). The R

value indicates that there is a linear correlation between concentration and absorbance, and almost all points lie on a straight line with a positive gradient [11]. Based on regression calculations from the standard curve, the values obtained are a (intercept) = -0.0009; b (slope) = 0.0742; and the linear equation is  $y = 0.0742x - 0.0009$  with a coefficient of determination ( $R^2$ ) of 1. The y coefficient represents absorbance, while x is the concentration of the methyl orange solution. The regression values obtained indicate a correlation between concentration and absorbance

### 3.3.2 Effect of pH

The determination of the optimum pH is carried out because the pH of the solution will influence the activity of functional groups on the adsorbent during the adsorption process. pH changes can affect the chemical properties and surface characteristics of the adsorbent, the solubility of the adsorbate, and the competition of ions in the adsorption process [12].

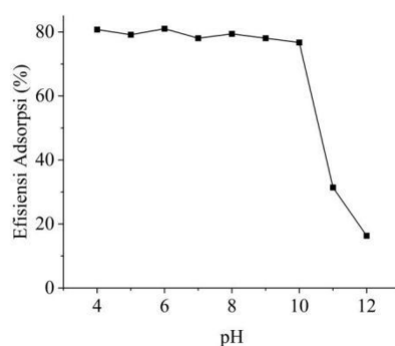


**Figure 3.** Curve of pH effect on the adsorption of methyl orange by Co/Fe-CO<sub>3</sub> hydrotalcite

Based on Figure 3, under pH conditions ranging from 4 to 10, the amount of adsorbed dye tends to remain stable under acidic conditions. The adsorption efficiency of the methyl orange dye absorbed by the adsorbent does not show significant differences. The pH of the solution results in changes in the charge distribution on the adsorbent and the dye due to protonation and deprotonation reactions of functional groups [13]. Hydrotalcite has -OH functional groups originating from metal hydroxide bonds on the surface. The calculated optimum pH is at pH 6 with an adsorption efficiency of 81.011% and an adsorption capacity of 12.962 mg/g, while at pH 11-12, there is a tendency for a decrease in efficiency and the amount of adsorbed dye.

Methyl Orange is an anionic dye that contains sulfonate groups carrying negative charges. In a solution of methyl orange at low pH conditions, the excess of H<sup>+</sup> ions in the solution causes the -OH functional groups on the adsorbent's surface to undergo protonation, making them positively charged and causing the deprotonation of the sulfonate groups of methyl orange [14]. Meanwhile, functional groups on the surface of the adsorbent that are positively charged can interact with the negatively charged sulfonate (-SO<sub>3</sub><sup>-</sup>) groups of the methyl orange dye, forming strong bonds between the adsorbent and the dye [15].

On the other hand, at high pH, the adsorption process can still occur because the hydroxyl (-OH) groups originating from the adsorbent weakly interact with the amine groups from the dye. However, its adsorption capacity becomes smaller. This happens because at high pH, the excess hydroxyl ions will compete with the anionic molecules of the dye to occupy active sites on the adsorbent, resulting in a low adsorption capacity [16].

### 3.3.3 Effect of contact time



The determination of the optimum adsorption time is performed to understand the time required for the adsorbent to adsorb methyl orange solution optimally. The longer the contact time between the methyl orange solution and hydrotalcite adsorption, the more opportunities the active sites of the adsorbent have to bind the dye. However, when saturation is reached, the contact time no longer has an effect, leading to a decrease in adsorption capacity.

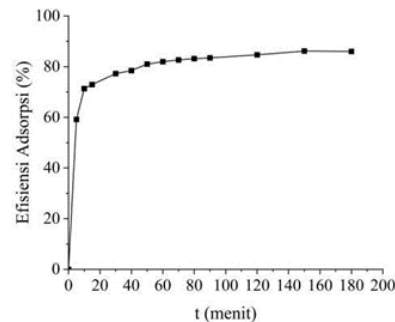


**Figure 4.** Curve of contact time effect on the adsorption of methyl orange by Co/Fe-CO<sub>3</sub> hydrotalcite

Based on Figure 4, the amount of adsorbed dye increases with increasing contact time in the range of 5-150 minutes. This is possible because at the beginning of the adsorption process, the adsorbent surface is still empty, so the amount of adsorbed dye increases rapidly. At a contact time of 60 minutes, the adsorption efficiency is 81.954%, and the adsorption capacity is 13.113 mg/g, indicating that the adsorbent's ability to adsorb methyl orange dye has reached equilibrium. This means that at this point, all active sites of the adsorbent have bound the adsorbate, so adding more time from 60 to 150 minutes does not significantly increase the amount of adsorbed dye.

However, at a contact time of 180 minutes, the adsorption capacity decreases. This is because the active sites on the adsorbent have reduced due to the possibility of the adsorbed dye being released back into the solution, forming a layer on the adsorbent's surface that covers the adsorbent layer, thereby reducing the adsorption efficiency [17].

### 3.3.4 Effect of LDH amount

The greater the mass of the adsorbent, the greater the efficiency of adsorbing methyl orange. This occurs because increasing the amount of adsorbent creates more empty space on the adsorbent's surface and active groups that can bind the adsorbate. This is evident in the range of adsorbent masses from 10 mg to 50 mg, where the adsorption capacity continues to increase. With an increase in the mass of the adsorbent, more empty spaces are provided on the adsorbent's adsorption sites to bind the adsorbate [18].

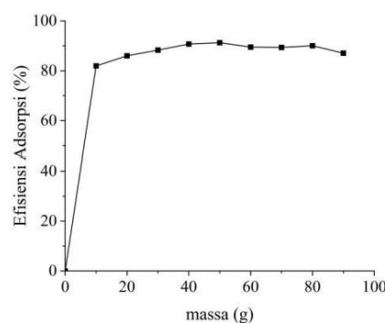


**Figure 5.** Curve of LDH amount effect on the adsorption of methyl orange by Co/Fe-CO<sub>3</sub> hydrotalcite

The data show that the optimum adsorption occurs at an adsorbent mass of 50 mg, with an adsorption percentage of 91.253% and an adsorption capacity of 2.920 mg/g. However, at adsorbent masses ranging from 60 to 90 grams, there is a decrease in adsorption efficiency, which can be attributed to the adsorbent surface reaching saturation, leading to a decrease in adsorption capacity [19].

### 3.3.5 Effect of adsorbate concentration

The influence of the initial dye concentration is based on the direct relationship between the dye concentration and the available active sites on the adsorbent's surface.

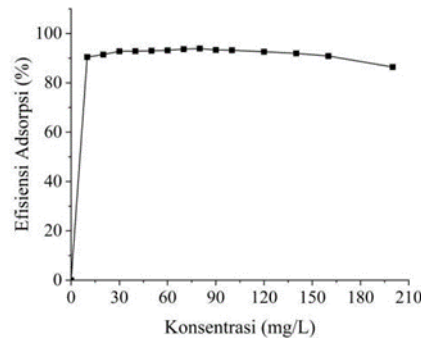


**Figure 6.** Curve of LDH amount effect on the adsorption of methyl orange by Co/Fe-CO<sub>3</sub> hydrotalcite

Optimum adsorption of methyl orange dye is achieved at a concentration of 80 mg/L with an adsorption efficiency of 93.903%. This indicates that after reaching the optimum conditions, an increase in the dye concentration no longer significantly affects the amount of dye adsorbed.

However, increasing the concentration of methyl orange dye will decrease the adsorption efficiency. This is because at higher concentrations, the amount of dye in the solution is not proportional to the number of adsorbent particles available, causing the hydrotalcite surface to reach saturation, and desorption or release of the adsorbate from the adsorbent may occur [20].

### 3.3.6 Adsorption kinetic

Adsorption kinetic is the ability of an adsorbent to adsorb by considering its reaction rate. The adsorption rate can be determined from the value of the adsorption rate constant ( $k$ ) and the reaction order, which refers to four adsorption kinetics equations.

**Table 1.** Kinetic Parameters of Methyl Orange Adsorption

Models Kinetics	Parameters		
	$R^2$	$k$ (g/mg.minute)	$q$ (mg/g)
First-order	0.8032	0.007	-
Second-order	0.8942	0.003	-
Pseudo-first-order	0.9570	0.023	3.163
Pseudo- second-order	0.9998	0.025	13.793

Based on Table 1, it can be observed that the  $R^2$  value for pseudo-second-order kinetics is greater compared to pseudo-first-order, first-order, and second-order kinetics. Therefore, the adsorption process of methyl orange dye by Co/Fe-CO<sub>3</sub> hydrotalcite follows pseudo-second-



order kinetics. The adsorption rate constant ( $k$ ) values indicate the speed of an adsorption process. The research results indicate that pseudo-second-order kinetics have the highest adsorption rate constant ( $k$ ) value. A higher adsorption rate constant value corresponds to a faster adsorption rate [21].

Furthermore, the data is supported by the adsorption capacity ( $q_e$ ) value in pseudo-second-order kinetics, which is 13.793 mg/g, closer to the experimental adsorption capacity ( $q_e$ ) value of 13.890 mg/g. This suggests that the adsorption rate is directly proportional to the available adsorbent capacity, but the adsorption rate decreases as it approaches equilibrium [22].

### 3.3.7 Adsorption isotherms

Adsorption isotherms describe the relationship between the amount of substance adsorbed by an adsorbent and the pressure or concentration at equilibrium at a specific temperature [23]. The data from the influence of methyl orange concentration in this study is used to determine adsorption isotherms and understand the adsorption process between hydrotalcite and the adsorbate, which is methyl orange. The isotherm models used in this research are the Langmuir and Freundlich isotherm models.

**Table 2.** Isotherm Parameters of Methyl Orange Adsorption

Langmuir Isotherm				Freundlich Isotherm			
$K_L$ (L/mg)	$q_{maks}$ (mg/g)	$R^2$	E (kJ/mol)	$K_F$ (mg/g)	n	$R^2$	E (kJ/mol)
0.084	35.461	0.858	6.132	3.073	0.781	0.9969	-2.781

Based on Table 2, the Langmuir isotherm yields a relatively high  $R^2$  value with a maximum adsorption capacity ( $q_{maks}$ ) of 35.461 mg/g. This indicates that the adsorption process of methyl orange dye by Co/Fe- $CO_3$  hydrotalcite occurs through chemical adsorption with the formation of a monolayer. Chemical interactions that can occur during this adsorption process include:

1. Electrostatic interactions between the anionic sulfate groups of methyl orange and the positively charged surface of Co/Fe- $CO_3$  hydrotalcite.
2. Hydrogen bonding between sulfate groups and hydroxyl groups on the surface of Co/Fe- $CO_3$  hydrotalcite.
3. Ion exchange processes between interlayer anions and anionic dye groups.

These interactions contribute to the adsorption of methyl orange by forming a monolayer on the hydrotalcite surface [24].

The  $R^2$  value for the Freundlich isotherm is higher than that for the Langmuir isotherm, indicating that the adsorption process follows the Freundlich adsorption isotherm more closely. The Freundlich isotherm assumes that adsorption occurs in a multilayer manner, and the active sites of the adsorbent are heterogeneous, meaning they have varying energy levels. The parameters in the Freundlich isotherm are the Freundlich constant ( $K_F$ ) and the adsorption intensity ( $n$ ). The Freundlich constant indicates the adsorbent's capacity to adsorb the adsorbate; the higher the value of  $K_F$ , the greater the adsorption capacity. The value of  $n$  is used to describe the adsorption process.

In this study, a value of  $n < 1$  was obtained, indicating that the adsorption of methyl orange by Co/Fe- $CO_3$  hydrotalcite involves chemical adsorption. The value of  $1/n$  in this study was found to be 1.2805, and  $1/n$  provides information about the strength of the adsorption process, where a value of  $1/n > 1$  indicates coordinative adsorption [25]. Based on these results, it can be inferred that during the adsorption process of methyl orange by Co/Fe- $CO_3$  hydrotalcite, both

physical and chemical interactions occur simultaneously. Figure 7, illustrates the possible coordinative adsorption that may occur in this study.

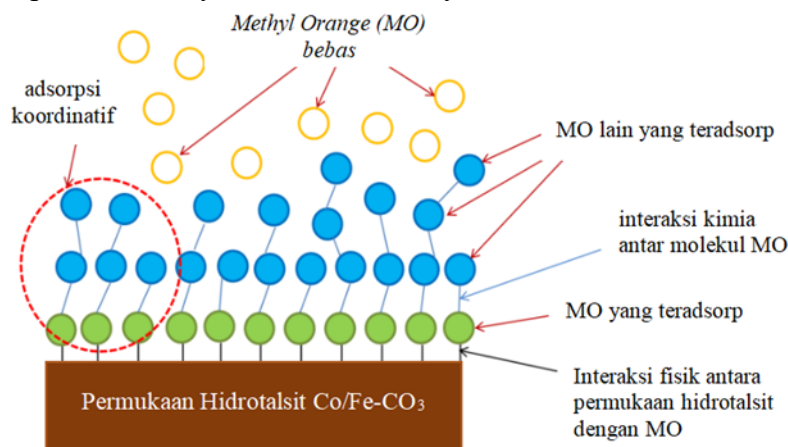


**Figure 7.** Illustration of coordinative adsorption

Based on Figure 7, physical interactions occur where methyl orange molecules directly adhere to the adsorbent's surface, forming a monolayer adsorption. In the second layer, chemical interactions occur between the adsorbed methyl orange molecules and free methyl orange molecules. The physical interaction between the adsorbent surface and methyl orange in the monolayer results in relatively weak interactions that are easily disrupted. The phenomenon of monolayer adsorption that forms indicates the presence of coordinative adsorption and chemical interactions among the adsorbates [26].

#### 4. Conclusion

The Co/Fe-CO<sub>3</sub> hydrotalcite has been successfully synthesized through coprecipitation and hydrothermal methods. The optimum adsorption conditions for methyl orange by Co/Fe-CO<sub>3</sub> hydrotalcite occur at pH 6, a contact time of 60 minutes, an adsorbent mass of 50 mg, and an optimum concentration of 80 mg/L. The adsorption process follows the pseudo-second-order kinetic model and the Freundlich isotherm.

#### References

- [1]. Gonawala, K. H., & Mehta, M. J. (2014). Removal Of Color From Different Dye Wastewater By Using Ferric Oxide As An Adsorbent. *Int J Eng Res Appl*, 4(5), 102-109.
- [2]. Chen, F., Wu, X., Bu, R., & Yang, F. (2017). Co-Fe hydrotalcites for efficient removal of dye pollutants via synergistic adsorption and degradation. *RSC advances*, 7(66), 41945-41954.
- [3]. Chen, F., Wu, X., Bu, R., & Yang, F. (2017). Co-Fe hydrotalcites for efficient removal of dye pollutants via synergistic adsorption and degradation. *RSC advances*, 7(66), 41945-41954.
- [4]. Liu, W., & Yu, Y. (2022). Ultrafast Advanced Treatment Of Chromium Complex-Containing Wastewater Using Co/Fe Layered Double Hydroxide. *Environmental Technology & Innovation*, 26, 102296.
- [5]. Iyi, N., Matsumoto, T., Kaneko, Y., & Kitamura, K. (2004). Deintercalation Of Carbonate Ions From A Hydrotalcite-Like Compound: Enhanced Decarbonation Using

- Acid– Salt Mixed Solution. *Chemistry Of Materials*, 16(15), 2926-2932.
- [6]. Ling, F., Fang, L., Lu, Y., Gao, J., Wu, F., Zhou, M., & Hu, B. (2016). A Novel CoFe Layered Double Hydroxides Adsorbent: High Adsorption Amount For Methyl Orange Dye And Fast Removal Of Cr (VI). *Microporous And Mesoporous Materials*, 234, 230-238.
- [7]. Bini, M., & Monteforte, F. (2018). Layered double hydroxides (LDHs): versatile and powerful hosts for different applications. *J. Anal. Pharm. Res.*, 7(1), 00206.
- [8]. Silva Neto, L. D., Anchietia, C. G., Duarte, J. L., Meili, L., & Freire, J. T. (2021). Effect of drying on the fabrication of MgAl layered double hydroxides. *ACS omega*, 6(33), 21819-21829.
- [9]. Drici-Setti, N., Lelli, P., & Jouini, N. (2020). LDH-Co-Fe-Acetate: A New Efficient Sorbent For Azoic Dye Removal And Elaboration By Hydrolysis In Polyol, Characterization, Adsorption, And Anionic Exchange Of Direct Red 2 As A Model Anionic Dye. *Materials*, 13(14), 3183.
- [10]. Ma, K., Cheng, J. P., Zhang, J., Li, M., Liu, F., & Zhang, X. (2016). Dependence of Co/Fe ratios in Co-Fe layered double hydroxides on the structure and capacitive properties. *Electrochimica Acta*, 198, 231-240.
- [11]. Nisah, K., & Nadhifa, H. (2020). Analisis Kadar Logam Fe Dan Mn Pada Air Minum Dalam Kemasan (AMDK) Dengan Metode Spektrofotometri Serapan Atom. *AMINA*, 2(1), 6-12.
- [12]. Wang, X., Shao, D., Hou, G., Wang, X., Alsaedi, A., & Ahmad, B. (2015). Uptake of Pb (II) and U (VI) ions from aqueous solutions by the ZSM-5 zeolite. *Journal of Molecular Liquids*, 207, 338-342.
- [13]. Nurhasni, N., Mar'af, R., & Hendrawati, H. (2018). Pemanfaatan Kulit Kacang Tanah (*Arachis hipogaea* L.) sebagai Adsorben Zat Warna Metilen Biru. *Jurnal Kimia VALENSI* Volume, 4(2).
- [14]. El Khanchaoui, A., Sajieddine, M., Mansori, M., & Essoumhi, A. (2022). Anionic dye adsorption on ZnAl hydrotalcite-type and regeneration studies based on “memory effect”. *International Journal of Environmental Analytical Chemistry*, 102(15), 3542-3560.
- [15]. Kyzas, G. Z. (2012). A decolorization technique with spent “Greek coffee” grounds as zero-cost adsorbents for industrial textile wastewaters. *Materials*, 5(11), 2069-2087.
- [16]. Conde MA, Liwaire CLS, Tchakounte AN, Ntinkam CAS, Nzugue DLE, Kede CM. (2020). Removal of methyl orange (MO) by chitosan modified by zero valent iron, *Int J Eng Res Technol*. 9(7), 1542–1549.
- [17]. Fitriansyah, A., Amir, H., & Elvinawati, E. (2021). Karakterisasi adsorben karbon aktif dari sabut pinang (*Areca catechu*) terhadap kapasitas adsorpsi zat warna indigosol blue 04-B. *Alotrop*, 5(1), 42-54.
- [18]. Yenti, S. R., Fadli, A., Nirwana, D., Fifiyana, R., & Sari, M. (2018). Model Keseimbangan Freundlich Pada Adsorpsi Ion Kadmium Menggunakan Hidroksiapatit. In *Prosiding Seminar Nasional Fisika Universitas Riau*, 3(2018).
- [19]. Fitriansyah, A., Amir, H., & Elvinawati, E. (2021). Karakterisasi adsorben karbon aktif dari sabut pinang (*Areca catechu*) terhadap kapasitas adsorpsi zat warna indigosol blue 04-B. *Alotrop*, 5(1), 42-54.



- [20]. Fillaeli, A., Siswani, E. D., Kristianingrum, S., Sulistyani, S., & Pratiwi, A. D. (2019). Adsorpsi Multilogam untuk Penurunan Kadar Cu, Fe, Ni dan Zn Menggunakan Arang Aktif Daun Pandan Laut. *Jurnal Sains Dasar*, 8(2), 64-69.
- [21]. Haryono, H. (2017). Analisa Kinetika Reaksi Pembentukan Kerak  $\text{CaCO}_3$  - $\text{CaSO}_4$  Dalam Pipa Beraliran Laminar Pada Suhu 30 oC dan 40 oC Menggunakan Persamaan Arrhenius. *TRAKSI*, 17(2).
- [22]. Hasan, A., Yerizam, M., & Yahya, M. H. (2021). Mekanisme Adsorben Zeolit Dan Manganese Zeolit Terhadap Logam Besi (Fe). *KINETIKA*, 12(1), 9-17.
- [23]. Ismadji, S., Soetaredjo, F. E., Santoso, S. P., Putro, J. N., Yuliana, M., Irawaty, W., ... & Lunardi, V. B. (2021). Adsorpsi pada fase cair: Keseimbangan, kinetika, dan termodinamika.
- [24]. Ismadji, S., Soetaredjo, F. E., Santoso, S. P., Putro, J. N., Yuliana, M., Irawaty, W., ... & Lunardi, V. B. (2021). Adsorpsi pada fase cair: Keseimbangan, kinetika, dan termodinamika.
- [25]. Kartika, S. E., & Amran, M. B. (2021). Sintesis dan Karakterisasi Poly (Anthranilic Acid-Co-Formaldehyde) untuk Adsorpsi Ion Pb (II). *ALCHEMY: Journal of Chemistry*, 9(1), 15-25.
- [26]. Nandiyanto, A. B. D., Ragadhita, R., & Yunas, J. (2020). Adsorption isotherm of densed monoclinic tungsten trioxide nanoparticles. *Sains Malaysiana*, 49(12), 2881-2890.